

Article

Electricity-Related Water Network Analysis in China Based on Multi-Regional Input–Output Analysis and Complex Network Analysis

Yiyi Zhang ^{1,*} , Huanzhi Fu ¹, Xinghua He ², Zhen Shi ¹, Tao Hai ¹, Peng Liu ³, Shan Xi ¹ and Kai Zhang ¹¹ Guangxi Power Transmission and Distribution Network Lightning Protection Engineering Technology Research Center, Guangxi University, Nanning 530004, China² SPIC Guangxi Electric Power Co., Ltd., Nanning 530004, China³ Guangxi Electric Power Grid Co., Ltd., Nanning 530004, China

* Correspondence: yiyizhang@gxu.edu.cn

Abstract: The transfer of electricity-related water across regions and sectors provides an opportunity to alleviate water stress and make the development of the power system sustainable. Yet, the key node identification and properties of the electricity-related water network have not been studied. In this study, the properties and key nodes of the regional sectoral electricity-related water network in China were analyzed based on a multi-regional input–output model and complex network analysis. An iterative method was proposed to calculate the water consumption index inventory. The results showed electricity transmission can affect the regional water consumption index. Degree, intensity, betweenness centrality, and closeness centrality indicators of nodes were used to identify the key nodes. Sector 24 in Shandong was the key node with the largest closeness centrality. Sector 9 in Xinjiang was the key node with the largest betweenness centrality. They were the best choice for establishing points to observe and control flows, respectively. The transfer network did not have the small-world nature with the average clustering coefficient being 0.478 and the average path length being 2.327. It is less likely to cause large-scale clustering change in the network. This study can provide references for the common sustainable development of power systems and water resources.



check for updates

Citation: Zhang, Y.; Fu, H.; He, X.; Shi, Z.; Hai, T.; Liu, P.; Xi, S.; Zhang, K. Electricity-Related Water Network Analysis in China Based on Multi-Regional Input–Output Analysis and Complex Network Analysis. *Sustainability* **2023**, *15*, 5360. <https://doi.org/10.3390/su15065360>

Academic Editors: Jiayu Xu, Meng Peng and Hongzhang Xu

Received: 28 November 2022

Revised: 18 February 2023

Accepted: 2 March 2023

Published: 17 March 2023



Copyright: © 2023 by the authors. Licensee MDPI, Basel, Switzerland. This article is an open access article distributed under the terms and conditions of the Creative Commons Attribution (CC BY) license (<https://creativecommons.org/licenses/by/4.0/>).

Keywords: electricity-related water; multi-regional input–output analysis; complex network analysis; iterative approximation; key nodes identification

1. Introduction

The water crisis has become widely concerning all over the world [1]. In China, there is a serious water crisis with half of the cities facing water shortages [2]. The per capita water resource available was only 2239.8 m³ in 2020 [3]. In addition, the spatial mismatch between water supply and demand do aggravate the water crisis [4]. In northern China, less than 20% of the water resource needs to sustain 47% of people [2]. Water scarcity is increasingly constraining Chinese sustainable development [5].

The power system consumed a large amount of water, which contributed to 14% of the total industrial water consumption [6]. With electricity demand increasing and water scarcity intensifying, a large number of thermal power and hydropower plants are faced with the risk of water shortage [7,8]. The water crisis has been a significant constraint factor for the development of power system. The study of electricity-related water is a key aspect of understanding the water limitation of the energy system, further reducing water shortages and providing policy strategies for the sustainable development of the power system.

Quantifying the water consumption of power generation is more than essential for studying the links between energy and water [9]. Process life cycle and hybrid life cycle analyses have been used to quantify water consumption for different types of power

generation. Liao et al. [10] calculated the water consumption of thermal power generation in China with plant-level data. Wang et al. [11] discussed and compared the water footprint of the five power types (hydro, thermal, solar, wind, and nuclear) based on life-cycle assessment. In addition, Xi et al. [12] established the hybrid water intensity inventory for power generation at the provincial level by considering the influence of power generation type, cooling technology, generator set, and other factors. Economic trade has led to lots of electricity and water consumption transfer. The electricity-related water transfer network has also been investigated at different levels, including the national level, the electricity grid level, and the provincial level. At the national level, Jin et al. [13] quantified virtual and physical water flows in China using information from 5408 generators and inter-provincial power transmission. At the electricity grid level, Zhu et al. [14] estimated the flows of virtual water and scarce water in the power system based on the water intensity method, but the spatial resolution of the study was not high. At the provincial level, Zhang et al. [15] investigated the evolution of the inter-provincial virtual water network from 2005 to 2014 based on an electricity transmission network.

The input–output table covers the production process and the usage of products. Input–output analysis (IO) can calculate the resource consumption for producing goods and services based on sectoral economic interactions [16,17]. It has been used to analyze environmental issues, including energy, carbon emission, water consumption and so on. Allan et al. [18] studied the economic and emissions impacts of the likely future development of the UK's offshore wind sector. Yang et al. [19] studied the structural emission reductions in China's industrial and energy systems in 2007–2015. Gao et al. [20] calculated the carbon footprint of China's coal-fired system using the environmental extended input–output model. Xie et al. [21] evaluated the carbon footprint among eight regions of China from a consumption-based perspective. Wu et al. [22] studied the direct and indirect water consumption efficiency and virtual water flow directions among different sectors based on the input–output model. Liao et al. [23] compared the water footprint for final energy demand in China's megacities to investigate the spatial impact of water scarcity. Chen et al. [9] quantitatively estimated the water footprint of each province in China and quantified the transfer of virtual water between provinces. The multi-regional input–output model (MRIO) was combined with the virtual water footprint to show how Australian agricultural demand affects water resources around the world [24]. To better study the properties and structure of the transfer networks, network analysis (e.g., ecological network analysis (ENA)) was combined with MRIO [16]. Wang et al. [25] studied the energy–water nexus of urban agglomeration based on MRIO and ENA. Zhang et al. [26] built the inter-provincial virtual water flows induced by electricity transmission in China and identified the control and dependence relationships using control and dependence allocation based on ENA. However, ENA mainly analyzes the network from the perspective of generalized ecological chain, and its help in the analysis of network characteristics and key nodes is limited.

Compared with ENA, complex network analysis (CNA) pays more attention to the structural properties of the network, the interaction among nodes, and the importance of nodes in a network from several different aspects like degree, intensity, closeness centrality, and betweenness centrality. Complex network theory is proposed and developed based on graph theory. It has been widely used in fields of society, economy, energy, and environment. For example, Wang et al. [27] studied the network risk propagation of agricultural supply chains based on CNA and analyzed the risk propagation on the network by using the Susceptible-Infected-Removed model. Liang et al. [28] identified the key sectors in the global virtual carbon transfer network for reducing carbon emissions in a targeted way. Ma et al. [29] The distribution structure of carbon emissions network among Chinese 28 sectors embodied in intermediate input were studied based on CNA. Wang et al. [30] calculated and compared the regional sectoral carbon dioxide transfer in China by combining complex network analysis and the hypothesis extraction method.

The existing research on electricity-related water focused more on the quantification and transfer relations. Few studies analyzed the network properties and identified the key

nodes in the electricity-related water transfer network. This study can be a supplement to the research blank of the distribution characteristics and identification of key nodes of electricity-related water network. The distribution of the degree and intensity of the nodes can help understand the structure and distribution characteristics of the network. It can give guidance at regional level to restrict or encourage policies for industries' electricity consumption. Using degree, intensity, closeness centrality, and between centrality indicators from CNA can identify the key nodes with special functions and further guide the optimization of electricity-related water network. For instance, the ability of nodes to observe and control flows in the network can be assessed by closeness centrality and betweenness centrality indicators, respectively. The key nodes identified by using these two indicators can provide references for the establishment of monitoring points and regulation points for electricity-related water networks. This study can provide references for the sustainable development of power systems and water resources.

In this study, the electricity-related water consumption index inventory considering the electricity transmission was proposed based on iterative approximation method. The electricity-related water transfer network among 30 regions and 27 sectors was constructed based on the environment-extended MRIO model. Combined with the CNA, the small-world nature of network and the properties of nodes were investigated. The key nodes were identified using out-degree, in-degree, out-intensity, in-intensity, closeness centrality, and betweenness centrality. The rest of the paper was organized as follows. Materials and methods were described in Section 2. The results were presented in Section 3. Finally, conclusions and the discussion were presented in Section 4.

2. Materials and Methods

2.1. Electricity-Related Water Consumption Index

According to the proportional sharing principle in power systems [31], the electricity ultimately consumed in an area is a mix of local generation and electricity from other regions. The mixing happens more than once in a complex power system. Electricity from other regions is also mixed locally and transmitted through transmission lines. When calculating the water consumption intensity from the perspective of consumption, it is necessary to consider the mixed effect of power transmission on the water consumption intensity of generation. An iterative process was proposed to represent the process of power from different regions being mixed in the system and arriving at the load, as shown in Figure 1.

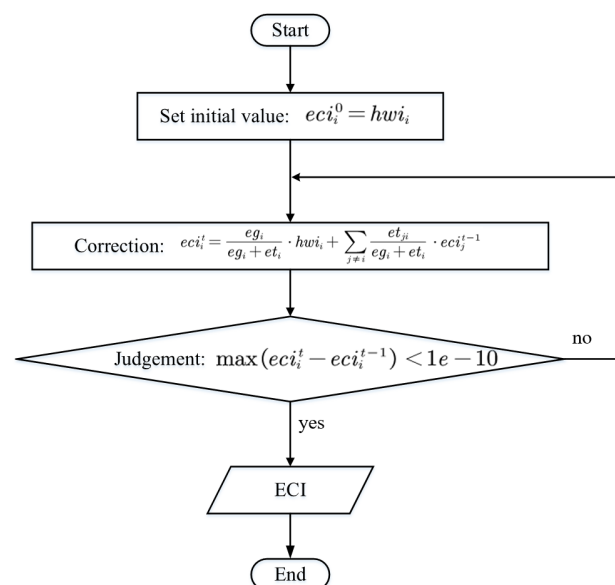


Figure 1. The calculation process of electricity-related water consumption index.

As for the electricity-related water consumption index, it can be modified iteratively according to the proportion of electric quantity until it meets the set error accuracy requirements. The error accuracy was set as 10^{-10} in this paper. The correction method is shown in Equation (1):

$$eti_i^t = \frac{eg_i}{eg_i + et_i} \cdot hwi_i + \sum_{j \neq i}^n \frac{et_{ji}}{eg_i + et_i} \cdot ect_j^{t-i} \quad (1)$$

where ect_i^t represents the electricity-related water consumption index of region i after the t iteration; eg_i represents the total power generation of region i ; et_i represents the total amount of electricity transmission into region i ; et_{ji} represents the amount of electricity transmission from region j to region i . The initial value of ect_i was set as the hybrid water consumption index of power generation in region i , which represents the state when there is no inter-region electricity transmission.

Due to the power generation structure in different regions having great differences, the water consumption intensity in different regions is also very different. We described the regional power generation water consumption intensity by using the hybrid water consumption intensity which is mixed by the five common types of power generation (hydropower, thermal, nuclear, wind, and solar power) according to the proportion of power generation. Its calculation method is shown as Equation (2):

$$hwi_i = \frac{eg_{i,k}}{eg_i} \cdot w_k \quad (2)$$

where hwi_i represents the hybrid water consumption index of power generation in region i ; $eg_{i,k}$ represents the amount of electricity generated by k_{th} technology in region i ; w_k represents the water intensity of k_{th} generation technology.

2.2. Construction of Electricity-Related Water Transfer Network

The electricity-related water transfer network was constructed based on MRIO. The original 42 sectors from input–output tables were grouped into 27 sectors for 30 regions in China, as shown in Table A1.

As an environmental extended coefficient, electricity-related water consumption was applied to the MRIO model. It was calculated according to the coefficient obtained in Section 2.1.

$$ewc_r^i = ect_i \cdot ec_r^i \quad (3)$$

where ewc_r^i represents the electricity-related water consumption of sector r in region i ; ect_i represents the electricity consumption of sector r in region i .

The direct environmental impact factor was defined as the amount of electricity-related water consumed per unit of total output, as shown in Equation (4):

$$ED = [ed_r^i], \quad ed_r^i = \frac{ewc_r^i}{x_r^i} \quad (4)$$

where ed_r^i represents the direct environmental impact index of sector r in region i ; x_r^i represents the total output of sector r in region i .

In the MRIO model framework, the direct consumption matrix can be expressed as:

$$A = [a_{r,s}^{i,j}], \quad a_{r,s}^{i,j} = \frac{z_{r,s}^{i,j}}{x_s^j} \quad (5)$$

where $a_{r,s}^{i,j}$ represents direct consumption index, which means the input from sector r in region i for per unit total output for sector s in region j ; $z_{r,s}^{i,j}$ represents intermediate input from sector r in region i to sector s in region j .

The total consumption coefficient matrix was used to allocate the consumption of a certain region and a certain sector. The matrix form of its calculation was shown as Equation (6).

$$L = (I - A)^{-1} \quad (6)$$

where L represents the complete consumption coefficient matrix; I represents the identity matrix.

Then, the complete environmental impact coefficient matrix was calculated by combining electricity-related water with trade relations, as shown in Equation (7):

$$ET = \hat{E}D \cdot L \quad (7)$$

The transfer network of electricity-related water can be built by Equation (8):

$$EWT = ET \cdot \hat{F} \quad (8)$$

where EWT represents the transfer relation matrix of electricity-related water, and \hat{F} represents the diagonal matrix of final consumption.

2.3. Complex Network Analysis

The electricity-related water transfer matrix was mapped to a weighted directed network. A sector of a region was mapped to a node, and a transfer relation was mapped to an edge whose weight was determined by the transition quantity. A total of 810 nodes and 307,223 edges were built in this study. The transfer matrix of electricity-related water was the adjacency matrix of the network. In addition, six indicators were chosen from different aspects to investigate the nodes with great importance in the network, which were out-degree, in-degree, out-intensity, in-intensity, closeness centrality, and betweenness centrality.

2.3.1. In-Degree and Out-Degree Analysis

Out-degree was the number of relations that electricity-related water outputs from the region and in-degree was the number of relations that electricity-related water inputs to the region. The calculation methods were shown in Equations (9) and (10):

$$kin_r = \sum_{s \neq r} l^{sr} \quad (9)$$

$$kout_r = \sum_{s \neq r} l^{rs} \quad (10)$$

where kin_r and $kout_r$ represent the in-degree and out-degree of node r , respectively; l^{sr} represents the number of edges from node s to node r .

2.3.2. Out-Intensity and In-Intensity Analysis

The out-intensity described the total amount of electricity-related water outflow of nodes, and the in-intensity described the total amount of electricity-related water inflow of nodes. The calculation methods were shown in Equations (11) and (12):

$$tin_r = \sum_{s \neq r} lw^{sr} \quad (11)$$

$$tout_r = \sum_{s \neq r} lw^{rs} \quad (12)$$

where tin_r and $tout_k$ are the in-intensity and out-intensity of node r ; lw^{sr} is the weight of the edge from node s to node r .

2.3.3. Closeness Centrality Analysis

Closeness centrality described the ability of node pairs to observe the flow of the network, and the node with the largest closeness centrality had the best observation field for the flow in the network. Closeness centrality can be calculated by the reciprocal of the average distance between nodes and all nodes in the network, as shown in Equation (13).

$$clc_r = \frac{N}{\sum_{s=1, s \neq r}^N pd_{sr}} \quad (13)$$

where clc_r represents the closeness centrality index of node r ; pd_{sr} represents the distance of the shortest path from node s to node r .

2.3.4. Betweenness Centrality Analysis

Betweenness centrality described the ability of nodes to control the flow in the network. The node with greater mediation centrality had a stronger ability to control the flow in the network, which can be calculated by the number of the shortest path through the node, as shown in Equation (14):

$$becr_r = \sum_{s \neq r \neq t}^N \frac{sg_{st,r}}{sg_{st}} \quad (14)$$

where $becr_r$ represents the betweenness centrality index of node r ; sg_{st} represents the number of shortest paths from node s to node t ; $sg_{st,r}$ represents the number of shortest paths through node r in the shortest path from node s to node t .

2.3.5. Small-World Nature of the Network

A small-world nature means most nodes are not adjacent to each other but can be indirectly connected through multiple paths in the network [30]. The small-world nature was determined by the average clustering coefficient (ACC) and the average path length (APL). The clustering coefficient of a node was the proportion of the number of edges among all its adjacent nodes in the potential maximum number of edges, as shown in Equations (15) and (16):

$$CC_r = \frac{ae_r}{\frac{an_r(an_r-1)}{2}} \quad (15)$$

$$ACC = \frac{1}{N} \cdot \sum CC_r \quad (16)$$

where CC_r represents the clustering coefficient of node r ; ae_r represents all edges of node r actually; an_r represents the adjacent nodes of node r .

APL was the average of the shortest path length between any two nodes, which reflected the connectivity of the network, as shown in Equation (17):

$$APL = \frac{2}{N(N-1)} \cdot \sum pd_{sr} \quad (17)$$

The small-world quotient (SWQ) was used to quantitatively evaluate whether the network has a small-world nature, which can be calculated as Equation (18). SWQ greater than 1 indicated that the network has a small-world nature:

$$SWQ = \frac{ACC}{APL} \cdot \frac{APL_{ran}}{ACC_{ran}} = \frac{ACC}{APL} \cdot \frac{\frac{\ln(N)}{\ln(\bar{k})}}{\frac{\bar{k}}{N}} \quad (18)$$

where ACC_{ran} and APL_{ran} represent the ACC and APL of a random network with the same number of nodes and average degree, respectively.

2.4. Data Sources

The data used in this study is mainly as follows. (1) The provincial power generation data in 2017 was from the “China Electric Power Yearbook” [32,33]; (2) Water consumption is the water use that could not return to the original resources and not available for reuse. The water consumption coefficients for five types of power generation technologies are derived from Feng et al. [34]; (3) The MRIO table of 2017 in China used in this study is from Zheng et al. [35]; (4) Data of power consumption comes from the China Energy Statistical Yearbook [36].

Due to data limitations, we only calculated and analyzed 30 provinces and autonomous regions in China (Tibet, Hong Kong, Taiwan, and Macau are excluded because of lacking data).

3. Results and Discussion

3.1. Regional Electricity-Related Water Consumption Coefficients

Figure 2 shows the water consumption index and the structure of power generation. There were obvious regional differences in water consumption coefficient. The minimum ECI was Inner Mongolia (3.01 L/kWh), followed by Ningxia (3.09 L/kWh) and Hebei (3.11 L/kWh). There were five regions with ECI over 10 L/kWh, which were Sichuan (15.89 L/kWh), Yunnan (15.38 L/kWh), Hubei (11.27 L/kWh), Chongqing (10.18 L/kWh), and Qinghai (10.09 L/kWh). Compared with HWI, ECI showed a certain amount of increase or reduction in some regions because of the electricity transmission among regions. Qinghai reduced by 0.66 L/kWh (from 10.74 L/kWh to 10.09 L/kWh). Shanghai increased by 3.83 L/kWh (from 3.26 L/kWh to 7.09 L/kWh). Guangdong increased by 2.80 L/kWh (from 4.24 L/kWh to 7.04 L/kWh). Chongqing increased by 1.85 L/kWh (from 8.33 L/kWh to 10.18 L/kWh).

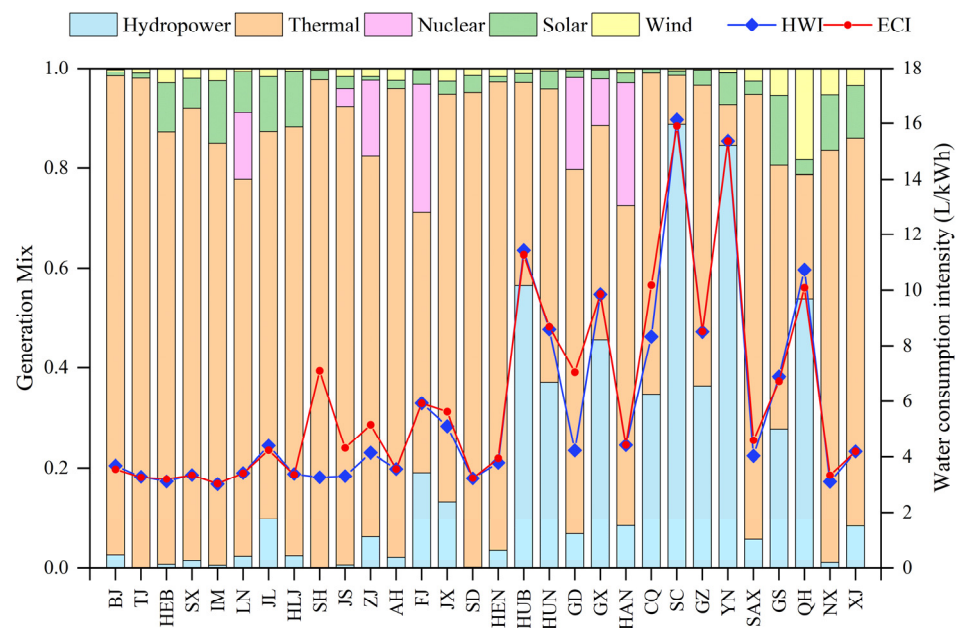


Figure 2. The regional electricity-related water consumption index and hybrid water intensity in 2017.

Figure 3 shows the regional electricity-related water consumption and water stress index (WSI) in 2017. Guangdong had the largest total electricity-related water consumption (337.00 Mm³), followed by Sichuan (254.79 Mm³). What is more, Jiangsu and Shandong had both large electricity-related water consumption and a large WSI. These regions need to pay more attention to the water crisis compared to Guangdong and Sichuan.



Figure 3. The regional electricity-related water consumption and water stress index in 2017.

3.2. Electricity-Related Water Transfer Network

The total transfer of electricity-related water was 75.36 billion m^3 in China in 2017. The transfer among regions and sectors is shown in Figure 4. The area of a circle represents the amount of electricity-related water passing through the node. The width of the line represents the amount of electricity-related water transferred through the path. The amount of electricity-related water flowing through different areas varied widely. The top five nodes were BJ-27 (6.11 billion m^3), JS-27 (4.68 billion m^3), GD-27 (4.42 billion m^3), JS-24 (3.82 billion m^3), and XJ-21 (3.49 billion m^3). There was also a huge difference in the amount of electricity-related water transferred through paths. The top five relations were from XJ-21 to ZJ-24 (238.66 Mm^3), from XJ-21 to CQ-24 (231.22 Mm^3), from XJ-21 to GD-27 (207.80 Mm^3), from ZJ-4 to JS-24 (183.87 Mm^3), and from XJ-21 to JS-27 (179.77 Mm^3).

Table 1 shows the regional inflow and outflow of electricity-related water. The largest inflow was to Guangdong (14.10 billion m^3), followed by Jiangsu (13.24 billion m^3) and Zhejiang (8.34 billion m^3). The largest outflow was from Xinjiang (7.33 billion m^3), followed by Qinghai (5.70 billion m^3) and Ningxia (4.3 billion m^3). The contribution of sectors in the inflow or outflow within the region is shown in Figure 5. As for the inflow, the contribution of the sectors presents obvious concentration characteristics. A large proportion of the inflow was in sector 24 (average 50.87%) and sector 27 (average 31.14%). The largest inflow sectors were sector 27 in Beijing (accounting for 88.61%) and sector 24 in Qinghai (accounting for 87.41%). As for the outflow, a large proportion of the outflow was in sector 14 (average 13.76%), sector 21 (average 13.58%), sector 22 (average 11.59%), and sector 4 (average 10.47%). The largest outflow sectors were sector 21 in Anhui (accounting for 52.14%) and sector 21 in Xinjiang (accounting for 47.65%).

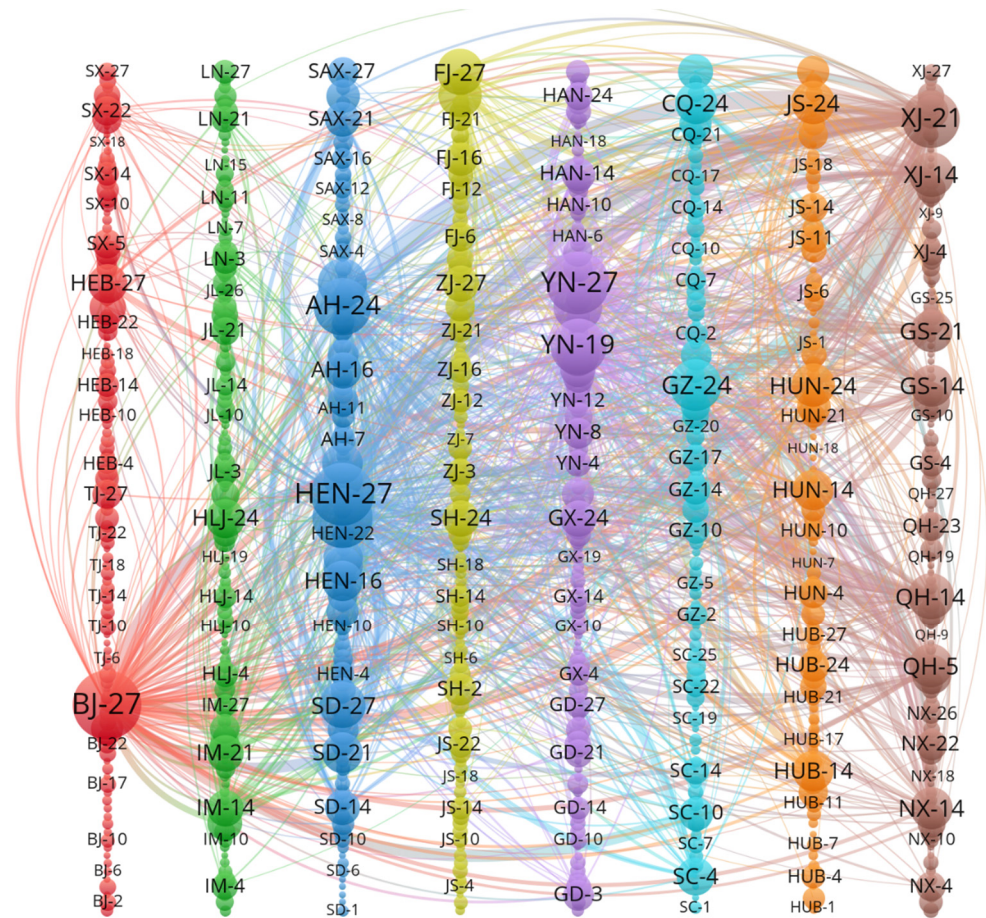


Figure 4. Electricity-related water transmission among regional sectors. (Note: The node name consists of region-sector, e.g., BJ-1 indicates sector 1 in Beijing).

Table 1. The Regional inflow and outflow of electricity-related water.

No.	Region	Inflow (Billion m ³)	Outflow (Billion m ³)
1	Beijing	6.89	0.58
2	Tianjin	0.76	0.62
3	Hebei	2.11	1.35
4	Shanxi	0.42	2.87
5	Inner Mongolia	0.64	4.12
6	Liaoning	1.51	1.57
7	Jilin	0.59	2.00
8	Heilongjiang	0.41	1.92
9	Shanghai	2.48	2.86
10	Jiangsu	13.24	1.39
11	Zhejiang	8.34	3.09
12	Anhui	1.61	1.33
13	Fujian	0.49	1.06
14	Jiangxi	1.06	1.83
15	Shandong	2.19	1.13
16	Henan	4.84	1.65
17	Hubei	0.74	2.19

Table 1. Cont.

No.	Region	Inflow (Billion m ³)	Outflow (Billion m ³)
18	Hunan	1.54	1.62
19	Guangdong	14.10	1.46
20	Guangxi	0.66	2.79
21	Hainan	0.13	2.76
22	Chongqing	3.35	2.71
23	Sichuan	2.22	1.88
24	Guizhou	0.60	3.12
25	Yunnan	1.68	3.51
26	Shannxi	2.10	2.24
27	Gansu	0.14	4.04
28	Qinghai	0.05	5.70
29	Ningxia	0.06	4.63
30	Xinjiang	0.41	7.33

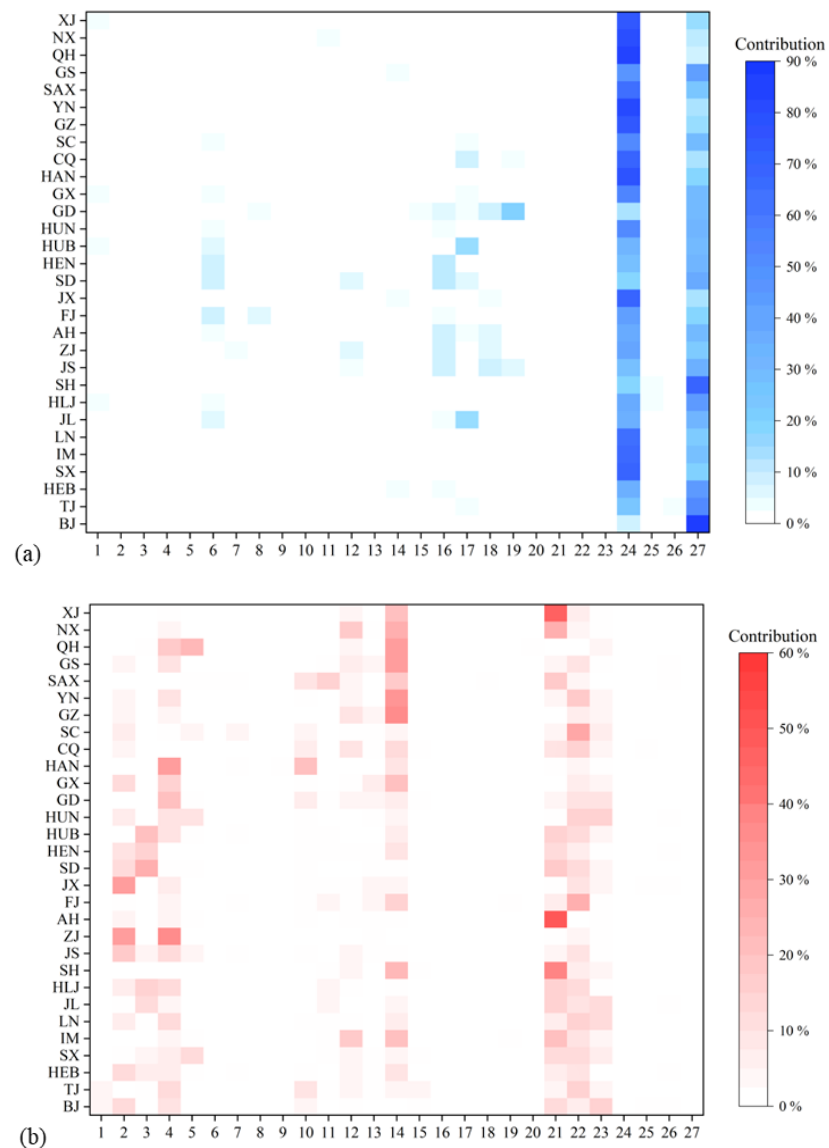


Figure 5. Sectoral contributions of inflows (a) and outflows (b) in 30 regions. (Note: The x-axis is the sector number, and the y-axis is the region).

3.3. Complex Network Analysis

The electricity-related water transfer network was calculated as a weighted directed network. A sector of a region was mapped to a node, and the transition relation was mapped to an edge, whose weight was determined by the transition quantity. The SWQ of the transfer network was 0.4947, with the ACC being 0.478 and APL being 2.327 in the network. Thus, the transfer network does not have an obvious small-world nature, which meant that the possibility of clustering changes in the network is very small. It was less likely to cause large-scale clustering change when some nodes or edges in the network changed.

The distribution of the in-degree of nodes is shown in Figure 6a. The maximum of the nodes' in-degree was 762, and the minimum was 0. The distribution of in-degree was very discrete, with all probabilities less than 0.65%, which meant that the distribution of node degrees is very discrete. The increasing rate of cumulative frequency varied at the point of in-degree was 335. The increase rate was larger when the in-degree was less than 335 and smaller when it was bigger than 335, which meant the average frequency in the range less than 335 was larger. The distribution of the out-degree of nodes is shown in Figure 6b. The maximum of the nodes' in-degree was 770, and the minimum was 0. The distribution of in-degree was very discrete as well. The increasing rate of cumulative frequency kept stable, with some slight fluctuations.

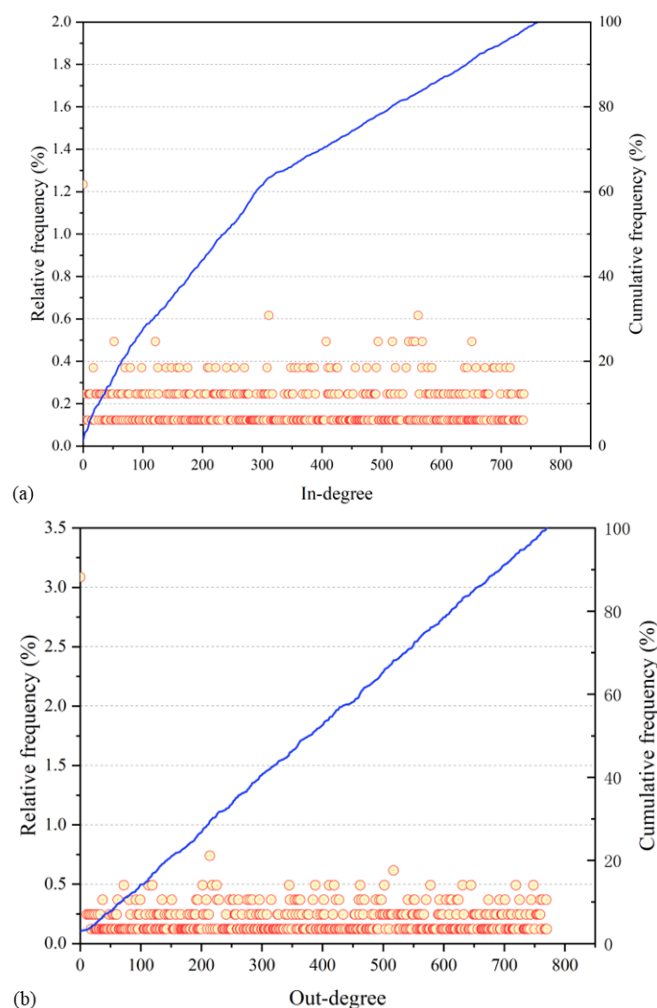


Figure 6. The distributions of in-degree (a) and out-degree (b) of nodes.

Figure 7 shows the distributions of the in-intensity and out-intensity of nodes. Both in-intensity and out-intensity showed a distribution with fewer at both ends and more

in the middle. More than 60% of the nodes were with the in-intensity from 0.01 Mm^3 to 50 Mm^3 . More than 60% of the nodes were with the out-intensity from 4 Mm^3 to 200 Mm^3 . However, the amount of electricity-related water transfer was concentrated on a few nodes with high intensity. The 18 nodes with in-intensity of more than 1000 Mm^3 transferred 58.87% of the total. The 12 nodes with out-intensity of more than 1000 Mm^3 transferred 23.127% of the total.

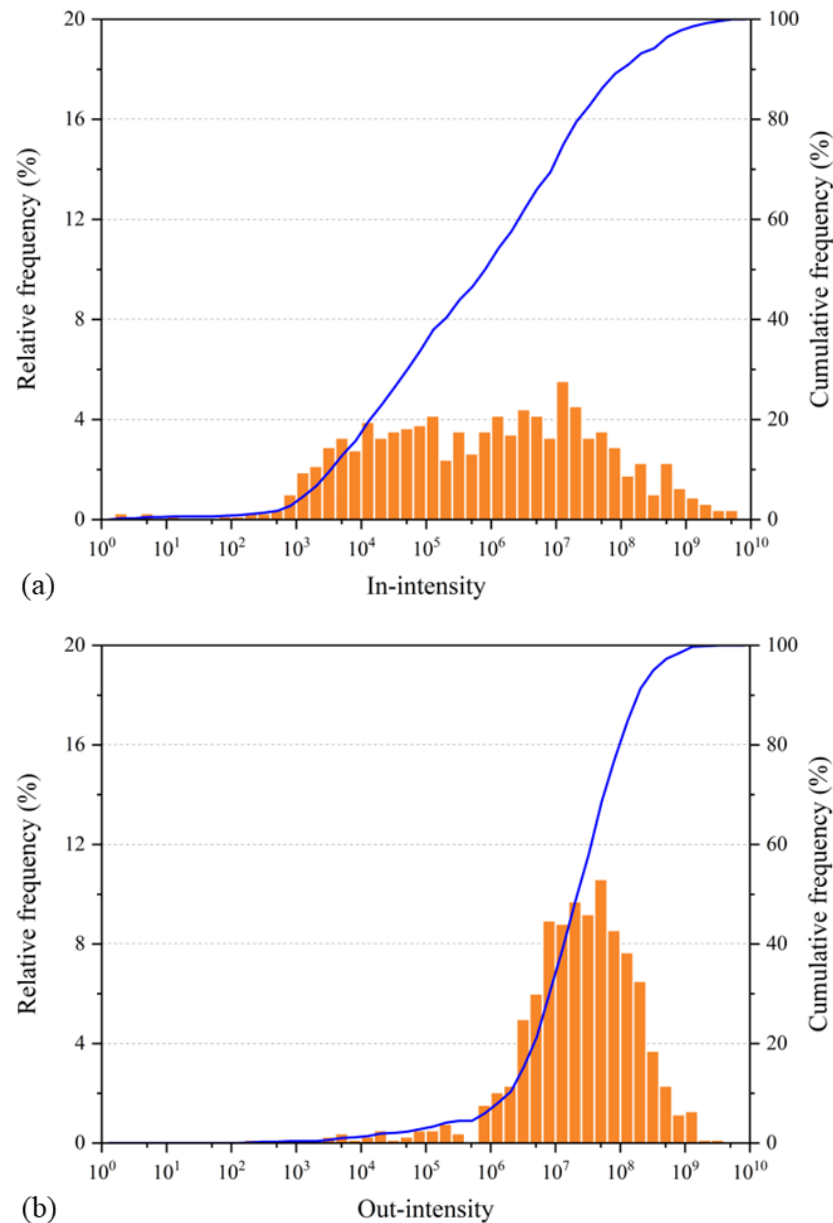


Figure 7. The distributions of in-intensity (a) and out-intensity (b) of nodes.

The correlations between degree and intensity of nodes were further analyzed, as shown in Figure 8. In order to better show the correlations between the more important (highly ranking) nodes, a logarithmic coordinate system was used to display the results. The in-intensity of the nodes with the top 10 in-degree was not very large. There was no strong correlation between the in-degree and the in-intensity of nodes. The main reason was that one or several transmission paths transferred a large amount of electricity-related water, and these paths with a large number of concentrated weights greatly increased the in-intensity or out-intensity of nodes. Taking sector 27 in Beijing with the largest in-intensity as an example, there were 18 paths' volumes above 50 Mm^3 , accounting for 2.36% of the

in-degree, but contributing 25.45% of the in-intensity. What is more, there was a similar relationship between the out-degree and the out-intensity of nodes.

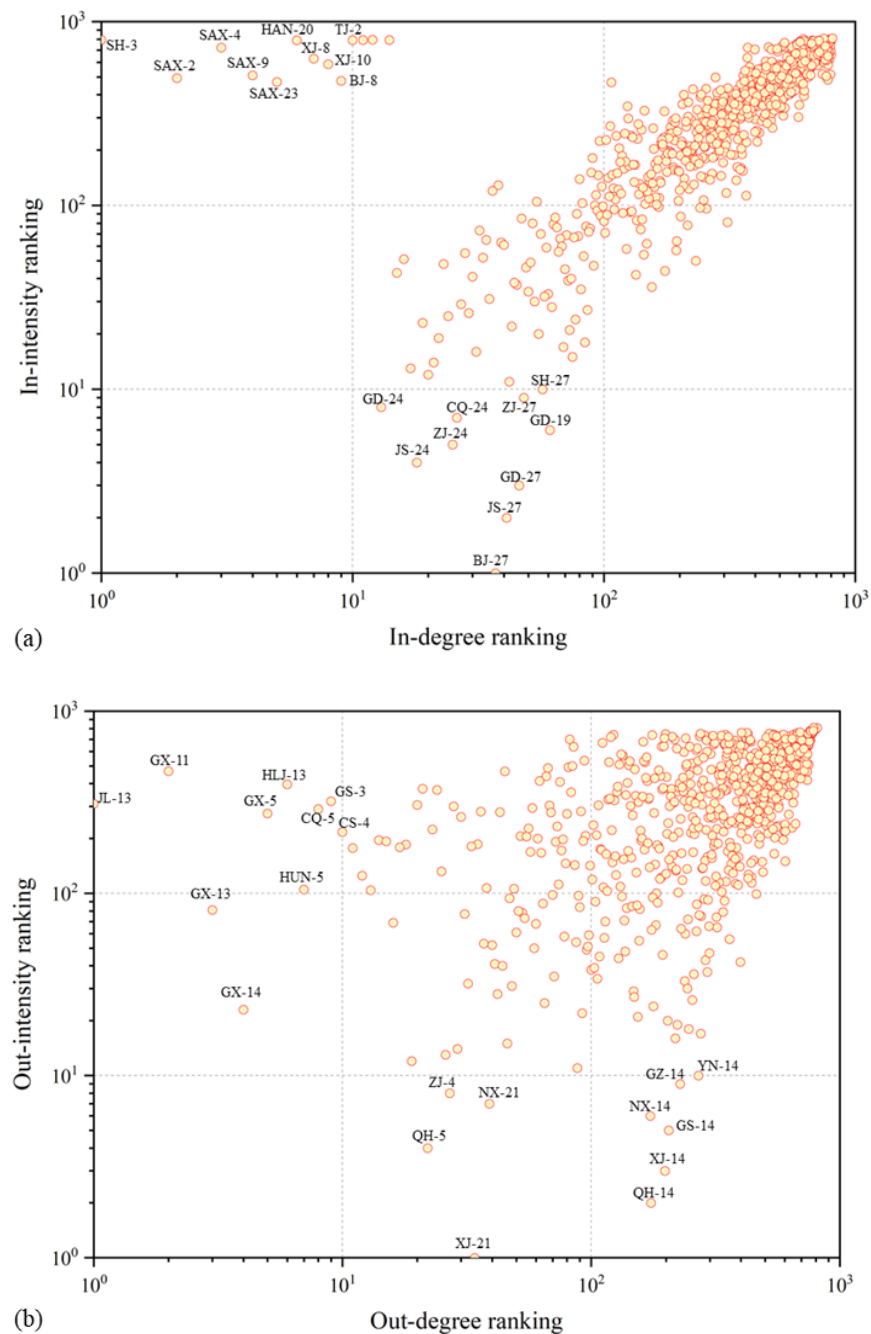


Figure 8. The correlations between in-degree and in-intensity of nodes (a), out-degree and out-intensity of nodes (b).

Figure 9a shows the distribution of closeness centrality of nodes. The nodes with the maximum closeness centrality were sector 24 in Shandong (1) and sector 24 in Guangdong (1), followed by sector 5 in Qinghai (0.97). These three nodes had the best view to observe the electricity-related water flow. Figure 9b shows the distribution of betweenness centrality. The nodes with the maximum betweenness centrality were sector 9 in Xinjiang (1), followed by sector 24 in Hainan (0.88) and sector 24 in Liaoning (0.85). Sector 9 in Xinjiang had the best control over the flow of electricity-related water in the transfer network. These indicators evaluated the status of nodes in the network from different perspectives,

and the key nodes in the network from these perspectives were identified, as shown in Table 2. These key nodes can be prioritized when building a sustainable grid that considers water security.

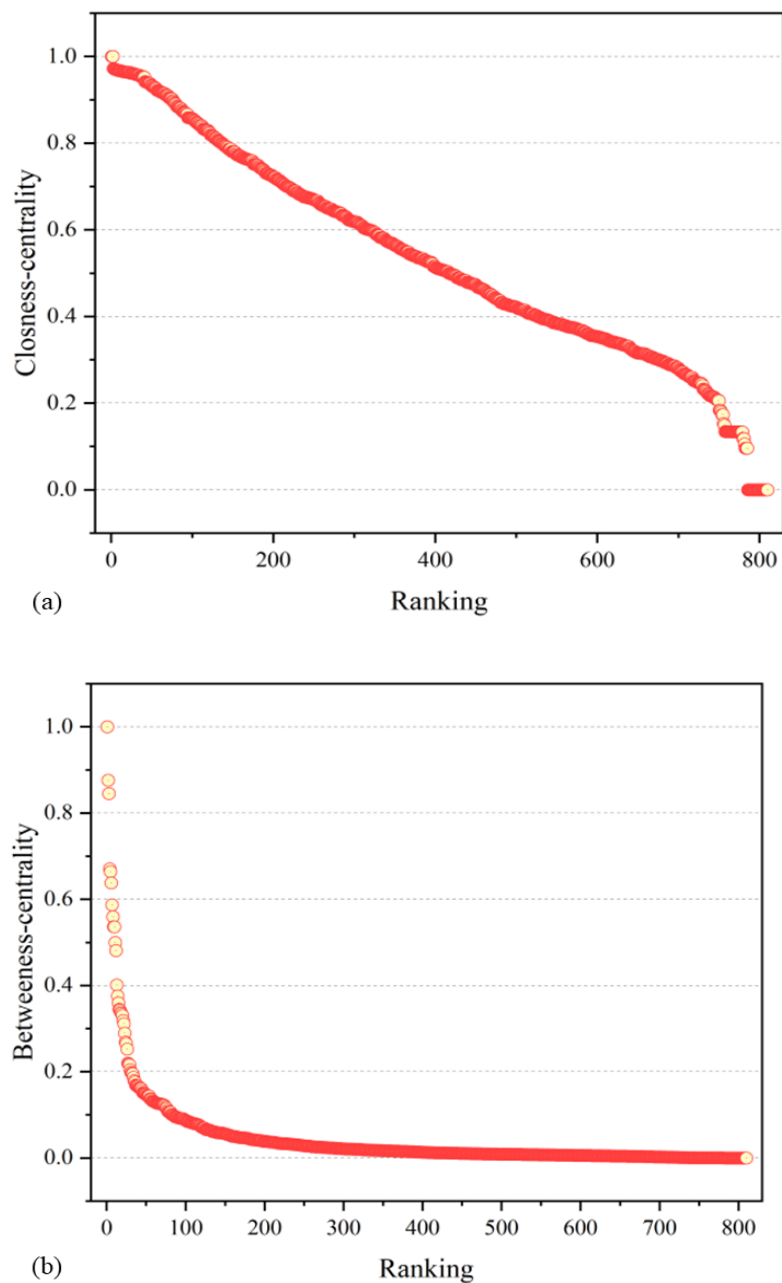


Figure 9. The distribution of closeness centrality (a) and betweenness centrality (b) of nodes.

Table 2. The top 5 key nodes in the network (Note: The node name consists of region-sector, e.g., SH-3 indicates sector 3 in Shanghai).

Indicators	1st	2nd	3rd	4th	5th
In-degree	SH-3	SAX-2	SAX-4	SAX-9	SAX-23
Out-degree	JL-13	GX-11	GX-13	GX-14	GX-5
In-intensity	BJ-27	JS-27	GD-27	JS-27	ZJ-24
Out-intensity	XJ-21	QH-14	XJ-14	QH-5	GS-14
Closeness centrality	SD-24	GD-24	QH-5	QH-23	QH-4
Betweenness centrality	XJ-9	HAN-24	LN-24	JL-6	HLJ-9

3.4. Discussion

3.4.1. Electricity-Related Water Consumption Index

Regional electricity-related water consumption intensity was calculated with an iterative approximation method, considering the complex electricity transmission among regions. This not only calculated consumption coefficients more reasonably and closer to the actual but also provided a reference method for subsequent research in related fields. In the iterative process, the ECI of the power transmission source had a great influence on the ECI of the receiver. For example, Guangdong received a large amount of electricity from Guizhou, Yunnan, and Hubei. The water consumption intensity of power generation was relatively high in these three regions because of the high proportion of hydropower. This will lead to an actual increase in water consumption corresponding to the electricity consumed in Guangdong. It was more reasonable that Guangdong's ECI increased by 2.80 L/kWh.

The power system is developed to the direction of low carbon. The capacity and generation of power plants using clean energy is increasing rapidly. It is necessary to consider the water impact of power system while setting the goal of carbon emission reduction. Wind and solar power development should be prioritized over hydropower development, because hydropower consumes much more water than the others. There are abundant solar and wind energy available for development in northwest China, which is beneficial to alleviate the energy crisis and achieve sustainable development. The construction of transmission lines is also gradually improving. In particular, the construction of ultra-high voltage direct current transmission lines can efficiently transmit power over long distances. Increasing the ability of electricity transmission from the wind and solar resource-rich regions to high-energy-demand regions like the southeast coastal cities is effective to reduce local electricity-related water consumption intensity and mitigate the energy and water pressure.

3.4.2. Electricity-Related Water Transfer Network

The MRIO results showed that there are lots of electricity-related water transfers caused by economic trade. The total transfer of electricity-related water was 75.36 billion m³ in 2017, accounting for 42% of the total electricity-related water consumption. Sectoral contributions to electricity-related water transfers varied widely across regions ranging from 0 to 0.88. The relatively large outflow contribution was mainly by construction sector and other services sector. The relatively large inflow contribution was mainly by the mining and processing of metal ores sector, the smelting and processing of metals sector, other manufacturing and waste resources sectors, and the production and distribution of electric power and heat power sector. The main reason was that it was affected by regional economic industry distribution and sectoral characteristics. The concentration of sectoral contributions provides direction for improving the electricity-related water network. The corresponding incentive policies can effectively promote the technological upgrading of these sectors with large outflow contributions, which can help improve energy utilization efficiency and reduce energy and water pressure.

3.4.3. Key Nodes Identification and Network Distribution Characteristics

Combining with complex network analysis, we found that the electricity-related water transfer network does not have a small-world nature ($SWQ < 1$), which meant that it was less likely to cause large-scale clustering change when some nodes or edges change. One possible influencing factor was that there are some nodes and paths with a large amount of virtual water transfer in the network. When these nodes and paths changed, they may affect the entire network and cause chain changes, and also suppressed the chain changes when the nodes and paths with small amount transfer change. Furthermore, there was a weak correlation between the degree and intensity of a node. The degree described the number of nodes connected to other nodes. Some nodes had many connections with other nodes, but the weight of the connection path was very small, resulting in a large degree

and a small strength. On the contrary, there were also one or several paths with a large weight, which resulted that connected nodes having large intensities and small degrees.

In addition, we used out-degree, in-degree, out-intensity, in-intensity, closeness centrality, betweenness centrality indicators to identify key nodes in the network. These key nodes can provide a good reference for policy designation to stabilize and improve electricity-related water network. The key nodes sector 3 in Shanghai, sector 2 in Shaanxi, and sector 4 in Shaanxi with the largest in-degree had the most inflow paths. The key nodes sector 13 in Jilin, sector 11 in Guangxi, and sector 13 in Guangxi with the largest out-degree had the most outflow paths. These nodes have strong stability in the network. These nodes can be the preferred choice for establishing transit or connections in the network.

The key nodes sector 27 in Beijing, sector 27 in Jiangsu, and sector 27 in Guangdong with the largest in-intensity maintained the stability of inflow. It was very important to ensure the stability of the transfer network. The transfer of electricity-related water can be more reasonable and efficient by optimizing the source and path of inflow. The key nodes sector 21 in Xinjiang, sector 14 in Qinghai, and sector 14 in Xinjiang with the largest out-intensity bore a lot of output pressure. It was very meaningful to improve the technical level of the corresponding industry to reduce water consumption. These nodes are better choices for supply-driven or demand-driven network optimization.

The key nodes sector 24 in Shandong, sector 24 in Guangdong, and sector 5 in Qinghai with the largest closeness centrality had the best view to observe the flow of electricity-related water in the network. Setting up observation points in these places can timely and efficiently observe the flow of electricity-related water for timely adjustment of relevant policies. The key nodes sector 9 in Xinjiang, sector 24 in Hainan, and sector 24 in Liaoning with largest betweenness centrality had a greater ability to subjectively control the flow of electricity-related water, and can effectively adjust the transfer path and the structure of the network. It was very difficult to master the strength and flow information of all nodes. These key nodes can observe and adjust the network state with limited human and material resources, even dynamic adjustment. Regardless, through the utilization of key nodes, policies to limit or encourage formulated for the regional sectors will better improve the overall network, not just the nodes.

The source of primary energy and the environment impact are likely to be major challenges for future power system. The water resource is not only one of the necessary resources of power system, but also one of the environmental impacts of power system. The stability of the electricity-related water network is important for the sustainable development of energy and water resources. The analysis of the characteristics and distribution characteristics of the network help us to understand the network structure and improve the network stability, such as increasing the degree of nodes with high output or input intensity or setting reserve paths for paths with high transfer volume. At the same time, key nodes help optimize the electricity-related water network from the perspectives of output, input, observation, and regulation of electricity-related water flow so as to avoid a potential water crisis threatening power grid security.

4. Conclusions

In this study, we analyzed the electricity-related water network based on the multi-region input–output model and complex network analysis. An iterative method was proposed to improve the accuracy of the water consumption index inventory. The transfer relationship and the sector contribution of regions were assessed. The small world nature and distribution characteristics of the network were investigated, and the key nodes in the network were identified based on out-degree, in-degree, out-intensity, in-intensity, closeness centrality, and betweenness centrality indicators. The conclusions are as follows:

Compared with HWI, the electricity-related water consumption index showed a certain change because of the electricity transmission among regions. The intensity increases in areas receiving electricity from areas with a high proportion of hydropower and decreases in areas receiving electricity from areas with a high proportion of wind and photovoltaic.

Increasing power output from areas with high wind and photovoltaic capacity could help improve the overall power-related water transfer network.

The contribution of the sectors presents obvious concentration characteristics. For inflow, a large proportion was in sector 24 (average 50.87%) and sector 27 (average 31.14%). For outflow, a large proportion was in sector 14 (average 13.76%), sector 21 (average 13.58%), sector 22 (average 11.59%), and sector 4 (average 10.47%).

The electricity-related water transfer network does not have a small-world nature. It is less likely to cause large-scale clustering change. Besides, there was no strong correlation between the in-degree and the in-intensity of nodes. The distribution of node degrees is very discrete with all probabilities less than 1%. More than 60% of the nodes were with the in-intensity from 0.01 Mm³ to 50 Mm³. More than 60% of the nodes were with the out-intensity from 4 Mm³ to 200 Mm³. There are a few paths that transmit large amounts of electricity-related water. Certain standards and limits should be set for these paths to avoid excessive concentration from destabilizing the transfer network and exacerbating potential water crises.

The key nodes identified were sector 3 in Shanghai with the largest in-degree and sector 13 in Jilin with the largest out-degree. These nodes can be the preferred choice for establishing transit or connections in the network. The key nodes identified were sector 27 in Beijing with the largest in-intensity, sector 21 in Xinjiang with the largest out-intensity. These nodes are better choices for supply-driven or demand-driven network optimization. The key nodes identified were sector 24 in Shandong with the largest closeness centrality, and sector 9 in Xinjiang with the largest betweenness centrality. These key nodes can observe and adjust the network state with less manpower and material resources.

Author Contributions: Conceptualization, H.F. and Y.Z.; Methodology, H.F. and Y.Z.; Investigation, H.F., K.Z. and S.X.; Writing—Original Draft, H.F.; Writing—Review & Editing, H.F., Y.Z., X.H., T.H. and Z.S.; Funding Acquisition and supervision, P.L. All authors have read and agreed to the published version of the manuscript.

Funding: This work was supported in part by the National Natural Science Foundation of China under Grant 52277138 and the Postdoctoral Science Foundation of China under Grant 2022MD713732.

Institutional Review Board Statement: Not applicable.

Informed Consent Statement: Not applicable.

Data Availability Statement: Not applicable.

Conflicts of Interest: The authors declare no conflict of interest.

Appendix A

Table A1. Sectors' compilation of regions.

Number	Aggregated 27 Sectors	Number	Original 42 Sectors
1	Agriculture, Forestry, Animal Husbandry and Fishery	1	Agriculture, Forestry, Animal Husbandry and Fishery
2	Mining and washing of coal	2	Mining and washing of coal
3	Extraction of petroleum and natural gas	3	Extraction of petroleum and natural gas
4	Mining and processing of metal ores	4	Mining and processing of metal ores
5	Mining and processing of nonmetal and other ores	5	Mining and processing of nonmetal and other ores
6	Food and tobacco processing	6	Food and tobacco processing
7	Textile industry	7	Textile industry
8	Manufacture of leather, fur, feather and related products	8	Manufacture of leather, fur, feather and related products
9	Processing of timber and furniture	9	Processing of timber and furniture

Table A1. Cont.

Number	Aggregated 27 Sectors	Number	Original 42 Sectors
10	Manufacture of paper, printing and articles for culture, education and sport activity	10	Manufacture of paper, printing and articles for culture, education and sport activity
11	Processing of petroleum, coking, processing of nuclear fuel	11	Processing of petroleum, coking, processing of nuclear fuel
12	Manufacture of chemical products	12	Manufacture of chemical products
13	Manuf. of non -metallic mineral products	13	Manuf. of non -metallic mineral products
14	Smelting and processing of metals	14	Smelting and processing of metals
15	Manufacture of metal products	15	Manufacture of metal products
16	Manufacture of purpose machinery	16	Manufacture of general purpose machinery
		17	Manufacture of special purpose machinery
17	Manufacture of transport equipment	18	Manufacture of transport equipment
18	Manufacture of electrical machinery and equipment	19	Manufacture of electrical machinery and equipment
	Manufacture of communication equipment, computers and other electronic equipment	20	Manufacture of communication equipment, computers and other electronic equipment
19	Manufacture of measuring instruments	21	Manufacture of measuring instruments
20	Other manufacturing and waste resources	22	Other manufacturing and waste resources
21	Production and distribution of electric power and heat power	24	Production and distribution of electric power and heat power
22	Production and distribution of gas and tap water	25	Production and distribution of gas
23		26	Production and distribution of tap water
24	Construction	27	Construction
25	Wholesale, retail trades, accommodation and catering	28	Wholesale and retail trades
26	Transport, storage, and postal services	30	Accommodation and catering
		29	Transport, storage, and postal services
		23	Repair of metal products, machinery and equipment
		31	Information transfer, software and information technology services
		32	Finance
		33	Real estate
27	others	34	Leasing and commercial services
		35	Scientific research
		36	Polytechnic services
		37	Administration of water, environment, and public facilities
		38	Resident, repair and other services
		39	Education
		40	Health care and social work
		41	Culture, sports, and entertainment
		42	Public administration, social insurance, and social organizations

References

- World Economic Forum. *Global Risks Report 2019*, 14th ed.; World Economic Forum: Geneva, Switzerland, 2019. Available online: <http://wef.ch/risks2019> (accessed on 25 November 2022).
- MWRC (Ministry of Water Resources of China). *China Water Resources Bulletin 2018*; Ministry of Water Resources of China: Beijing, China, 2019. (In Chinese)
- NBSC (National Bureau of Statistics of China). *China's Statistical Yearbook 2021*; National Bureau of Statistics of China: Beijing, China, 2021. (In Chinese)

4. Larsen, M.A.D.; Drews, M. Water use in electricity generation for water-energy nexus analyses: The European case. *Sci. Total Environ.* **2019**, *651*, 2044–2058. [[CrossRef](#)]
5. Ju, X. Research on Sustainable Development of Water, Energy and Food in China Based on System Dynamics. Master's Thesis, China University of Petroleum, Beijing, China, 2019. (In Chinese)
6. Cai, B.; Zhang, B.; Bi, J.; Zhang, W. Energy's thirst for water in China. *Environ. Sci. Technol.* **2014**, *48*, 11760–11768. [[CrossRef](#)]
7. Van Vliet, M.T.H.; Yearsley, J.R.; Ludwig, F.; Vögele, S.; Lettenmaier, D.P.; Kabat, P. Vulnerability of US and European electricity supply to climate change. *Nat. Clim. Chang.* **2012**, *2*, 676–681. [[CrossRef](#)]
8. Van Vliet, M.T.H.; Wiberg, D.; Leduc, S.; Riahi, K. Power-generation system vulnerability and adaptation to changes in climate and water resources. *Nat. Clim. Chang.* **2016**, *6*, 375–380. [[CrossRef](#)]
9. Chen, W.; Wu, S.; Lei, Y.; Li, S. China's water footprint by province, and inter-provincial transfer of virtual water. *Ecol. Indic.* **2017**, *74*, 321–333. [[CrossRef](#)]
10. Liao, X.; Hall, J.W.; Eyre, N. Water use in China's thermoelectric power sector. *Glob. Environ. Chang.* **2016**, *41*, 142–152. [[CrossRef](#)]
11. Wang, L.; Wang, Y.; Lee, L.C. Life cycle water consumption embodied in inter-provincial electricity transmission in China. *J. Clean. Prod.* **2020**, *269*, 122455. [[CrossRef](#)]
12. Xi, S.; Zhang, Y.; Liu, J.; Zhang, C.; Zhang, K.; Wang, J. Evolution of interprovincial virtual water flows along with electricity. *J. Clean. Prod.* **2021**, *322*, 128957. [[CrossRef](#)]
13. Jin, Y.; Behrens, P.; Tukker, A.; Scherer, L. The energy-water nexus of China's interprovincial and seasonal electric power transmission. *Appl. Energy* **2021**, *286*, 116493. [[CrossRef](#)]
14. Zhu, X.; Guo, R.; Chen, B.; Zhang, J.; Hayat, T.; Alsaedi, A. Embodiment of virtual water of power generation in the electric power system in China. *Appl. Energy* **2015**, *151*, 345–354. [[CrossRef](#)]
15. Zhang, Y.; Hou, S.; Liu, J.; Zheng, H.; Wang, J.; Zhang, C. Evolution of Virtual Water Transfers in China's Provincial Grids and Its Driving Analysis. *Energies* **2020**, *13*, 328. [[CrossRef](#)]
16. Zhang, Y.; Zheng, H.; Yang, Z.; Li, Y.; Liu, G.; Su, M.; Yin, X. Urban energy flow processes in the Beijing–Tianjin–Hebei (Jing–Jin–Ji) urban agglomeration: Combining multi-regional input-output tables with ecological network analysis. *J. Clean. Prod.* **2016**, *114*, 243–256. [[CrossRef](#)]
17. Cazarro, I.; Duarte, R.; Sánchez Chóliz, S. Multiregional input-output model for the evaluation of Spanish water flows. *Environ. Sci. Technol.* **2013**, *47*, 12275–12283. [[CrossRef](#)]
18. Allan, G.; Comerford, D.; Connolly, K.; McGregor, P.; Ross, A.G. The economic and environmental impacts of UK offshore wind development: The importance of local content. *Energy* **2020**, *199*, 117436. [[CrossRef](#)]
19. Yang, J.; Dong, H.; Jiang, T. Structural emission reduction in China's industrial systems and energy systems: An input-output analysis. *Environ. Sci. Pollut. Res.* **2022**, *29*, 6010–6025. [[CrossRef](#)]
20. Gao, T.; Jin, P.; Song, D.; Chen, B. Tracking the carbon footprint of China's coal-fired power system. *Resour. Conserv. Recycl.* **2022**, *177*, 105964. [[CrossRef](#)]
21. Xie, X.; Cai, W.; Jiang, Y.; Zeng, W. Carbon Footprints and Embodied Carbon Flows Analysis for China's Eight Regions: A New Perspective for Mitigation Solutions. *Sustainability* **2015**, *7*, 10098–10114. [[CrossRef](#)]
22. Wu, X.J.; Sun, J.; Liu, J.; Ding, Y.K.; Huang, G.H.; Li, Y.P. Ecological Network-based Input-output Model for Virtual Water Analysis in China. In *IOP Conference Series: Earth and Environmental Science*; IOP Publishing: Bristol, UK, 2020; Volume 435, p. 012010.
23. Liao, X.; Zhao, X.; Liu, W.; Li, R.; Wang, X.; Wang, W.; Tillotson, M.R. Comparing water footprint and water scarcity footprint of energy demand in China's six megacities. *Appl. Energy* **2020**, *269*, 115137. [[CrossRef](#)]
24. Ridoutt, B.G.; Hadjikakou, M.; Nolan, M.; Bryan, B. From water-use to water-scarcity footprinting in environmentally extended input-output analysis. *Environ. Sci. Technol.* **2018**, *52*, 6761–6770. [[CrossRef](#)]
25. Wang, S.; Chen, B. Energy–water nexus of urban agglomeration based on multiregional input-output tables and ecological network analysis: A case study of the Beijing–Tianjin–Hebei region. *Appl. Energy* **2016**, *178*, 773–783. [[CrossRef](#)]
26. Zhang, Y.; Hou, S.; Chen, S.; Long, H.; Liu, J.; Wang, J. Tracking flows and network dynamics of virtual water in electricity transmission across China. *Renew. Sustain. Energy Rev.* **2021**, *137*, 110475. [[CrossRef](#)]
27. Wang, X. Research on Agricultural Supply Chain Modeling and Network Risk Propagation Based on Complex Network. Ph.D. Thesis, Jilin University, Jilin, China, 2017. (In Chinese)
28. Liang, S.; Feng, Y.; Xu, M. Structure of the global virtual carbon network: Revealing important sectors and communities for emission reduction. *J. Ind. Ecol.* **2015**, *19*, 307–320. [[CrossRef](#)]
29. Ma, N.; Li, H.; Tang, R.; Dong, D.; Shi, J.; Wang, Z. Structural analysis of indirect carbon emissions embodied in intermediate input between Chinese sectors: A complex network approach. *Environ. Sci. Pollut. Res.* **2019**, *26*, 17591–17607. [[CrossRef](#)]
30. Wang, Y.; Lei, Y.; Fan, F.; Li, L.; Liu, L.; Wang, H. Inter-provincial sectoral embodied CO₂ net-transfer analysis in China based on hypothetical extraction method and complex network analysis. *Sci. Total Environ.* **2021**, *786*, 147211. [[CrossRef](#)]
31. Bialek, J. Tracing the flow of electricity. *IET Proc. Gener. Transm. Distrib.* **1996**, *143*, 313–320. [[CrossRef](#)]
32. CEC (China Electricity Council). *China Electric Power Yearbook 2017*; China Electricity Council: Beijing, China, 2017. (In Chinese)
33. NBSC (National Bureau of Statistics of China). *China Statistical Yearbook 2017*; National Bureau of Statistics of China: Beijing, China, 2017. (In Chinese)
34. Feng, K.; Hubacek, K.; Siu, Y.L.; Li, X. The energy and water nexus in Chinese electricity production: A hybrid life cycle analysis. *Renew. Sustain. Energy Rev.* **2014**, *39*, 342–355. [[CrossRef](#)]

35. Zheng, H.; Bai, Y.; Wei, W.; Meng, J.; Zhang, Z.; Song, M.; Guan, D. Chinese provincial multi-regional input-output database for 2012, 2015, and 2017. *Sci. Data* **2021**, *8*, 244. [[CrossRef](#)]
36. NBSC (National Bureau of Statistics of China). *China Statistical Yearbook 2020*; National Bureau of Statistics of China: Beijing, China, 2020. (In Chinese)

Disclaimer/Publisher's Note: The statements, opinions and data contained in all publications are solely those of the individual author(s) and contributor(s) and not of MDPI and/or the editor(s). MDPI and/or the editor(s) disclaim responsibility for any injury to people or property resulting from any ideas, methods, instructions or products referred to in the content.